INFLUENCE OF RESIDUAL STRESS ON FATIGUE STRENGTH OF CARBURIZED AND SHOT PEENED NOTCHED SPECIMENS

K. Ogawa, H. Yamada and K. Saruki, Toyota Central R&D Labs., Inc.
and
M. Yokoi and M. Inuzuka, Toyota Motor Corp., Japan

ABSTRACT

Bending fatigue tests were carried out on gears and three differently notched specimens simulating gear-tooth root, which were shot-peened under different conditions without machining after heat treatment. The results indicated that the fatigue strengths of shot-peened specimens and gears were strongly affected by the residual stresses beneath the surface, though not so much by the changes in the hardness and surface roughness induced by shot peening. The correlation between the fatigue limits and the residual stresses was also examined using a simple model based on the critical depth criterion. Assuming the critical depth influencing fatigue properties to be 0.05 mm, the fatigue limits of shot-peened specimens with different notch-radiuses correlated well with the residual stresses induced by shot peening.

KEYWORDS

shot peening, fatigue strength, carburizing, notched specimen, helical gear, residual stress, oxidation layer, critical depth, stress gradient

INTRODUCTION

Shot peening is widely used for the improvement of the fatigue properties of carburized gears in the recent automobile industry[1-4]. Investigations indicated that the main factor in the fatigue strength improvement was the compressive residual stresses induced by shot peening[5-7]. However, there are few investigations concerning the correlation between the fatigue strengths and residual stresses of the notched parts such as gear-tooth root[7,8]. The initiation points of fracture on the carburized gears are mostly at the surface of the tooth root, though the stress gradient into depth varies with the root radius.

This study investigates the correlation between the fatigue strengths and the change in the material state of shot-peened gears and specimens with different notch-radiuses. Furthermore, the influence of residual stress on the fatigue limit was examined using a simple model based on the critical depth criterion which NEUBER proposed.

EXPERIMENTAL PROCEDURES

Material, Specimens and Gears

The material used for the tests is JIS SCr420 steel of which chemical composition is given in Table I. The specimens with three different notch-radiuses ρ and stress concentration factors Kt were fabricated from the material as indicated in Fig. 1. The specimens were gas-carburized in a pusher type furnace, and then quenched in oil. The objective case depth 0.6 mm at 550 Hv was chosen. As for the gears, tested were the helical gears with normal module 2.25, normal pressure angle 22.5°, helix angle 28°, pitch circle diam. 117 mm, number of teeth 46, and face width 15.4 mm. The gears were carburized under the conditions similar to those of the specimens.

Shot Peening Treatments

The specimens and the gears were shot-peened with an impeller type shot peening machine under three different conditions, SP-A, SP-B, and SP-C, without machining after heat-treatment, as summarized in Table II.

Residual Stress Measurements

The residual stresses of specimens were determined by the X-ray method, so-called the $\sin^2\psi$-method. The conditions for the residual stress measurement are summarized in Table III. The notched specimens were measured on their flat surface just beside the notch root in the longitudinal direction. In the case of gears, they were measured at the tooth bottom, parallel to the tooth. The depth profiles of residual stress were determined by stepwise thin layer removals.

Fatigue Tests

Fatigue tests for the notched specimens were carried out with an electromagnetic resonance type fatigue testing machine in the bending mode with a stress ratio R ($=\sigma\min/\sigma\max$) of 0 and a frequency of 70 Hz. Fatigue tests for gears were performed with the resonance type gear fatigue tester[9] illustrated in Fig. 2. The test torques of the sinusoidal wave with a stress ratio R of 0 and a frequency of 40 Hz were loaded to a pair of meshed gears, one of which was held stationary to a load cell, and the other, fastened to a vibrating

Table I Chemical composition (wt%)

C	Si	Mn	P	S	Cu	Ni	Cr
0.19	0.24	0.69	0.024	0.014	0.18	0.07	1.02

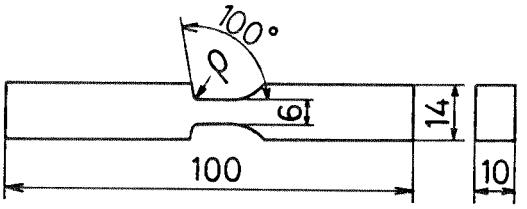

Notch rad. ρ, mm	Stress conc. factor, Kt
0.5	2.02
1.0	1.59
2.0	1.36

Fig. 1 Shape and dimensions of specimens.

Table II Conditions of shot peening

Condition	Shot type	Shot diam. (mm)	Shot hardness (Hv)	Peripheral speed of impeller (m/s)	Exposure time (min.)
SP-A	steel ball	0.8 (0.6)*	450	61	3
SP-B			580	70	
SP-C			700	50	

* only for specimens with notch radius 0.5 mm

Table III conditions of X-ray stress measurement

Characteristic X-ray	Cr-Kα
Diffraction Plane	Fe(211)
Tube voltage, kV	30
Tube current, mA	8
Irradiated area, mm^2	1×3
Incident beam angle, °	0, 25, 35, 45
Counter	PSPC

shaft, oscillating against the stationary gear.

RESULTS

Microstructure, Hardness, Residual Stress, and Surface Roughness

Microphotographs of a carburized specimen and a specimen shot-peened after carburizing are shown in Fig. 3. The oxidized and non-martensitic layer is observed near the surface of both specimens. The maximum depth of the layers was about 25 μm, regardless of peened or not. The hardness and residual stress distributions are shown in Figs. 4 and 5, respectively. The hardnesses near the surface are slightly increased by shot peening. The residual stresses, on the other hand, show a remarkable change. For the specimens with the notch-radius of 1.0 mm, the maximum compressive stresses exist at the depth of 0.04 - 0.05 mm from the surface under all shot peening conditions. The surface roughness was 2 μm Rmax for the as-carburized specimens, and 6, 7, and 8 μm Rmax for the specimens shot-peened under the conditions, SP-A, SP-B, and SP-C, respectively. The difference was small between the shot-peened specimens.

S-N curves

Notched Specimens. The S-N curves of the carburized and the shot-peened specimens with the notch-radius ρ of 0.5, 1.0, and 2.0 mm are shown in Fig. 6. The fatigue limits for specimens with ρ = 0.5, and 2.0 mm increased with the intensity of shot peening. However, the fatigue limits of specimens with ρ = 1.0 mm under the shot peening conditions SP-A and SP-B fell below that of the carburized specimen. This seems to be due to the slight difference in the lots used for the heat-treatment of the specimens with ρ = 0.5, and 2.0 mm and those with ρ = 1.0 mm.

Gears. The S-N curves of the as-carburized and shot-peened gears are shown in Fig. 7. The initiation points of fracture were at the tooth root for all tested gears. Shot peening increases the fatigue strengths of gears. The gears shot-peened under the condition SP-C increased the fatigue limit by 43% compared with the as-carburized gears.

DISCUSSION

The fatigue strengths of carburized and shot-peened notched specimens were affected by the material states near the surface, particularly by the oxidized and non-martensitic layer, the hardness and residual stress distributions, and the surface roughnesses. In this experiment, there were no changes in the thickness of the oxidized layer by shot peening.

The hardness near the surface of shot-peened specimens was only 50 - 80 Hv higher than those of the as-carburized, as shown in Fig. 4. The increases in fatigue strength do not correspond with the increases in hardness. The increase in hardness by shot peening is therefore considered to be a minor factor in the fatigue strength improvement.

The surface roughnesses of the shot-peened specimens were within 6 - 8 μm Rmax under all the tested shot peening conditions. Such a small variation in surface roughness has little effect on the fatigue strength.

On the other hand, it is evident that the variation in residual stress strongly affects the fatigue strength. Figure 8 shows the relation between the fatigue limit represented by $Kt \cdot \Delta\sigma w$ and the maximum compressive residual stress. The fatigue limits of the shot-peened specimens increase with compressive residual stress. However, it is noteworthy that the fatigue limits of the as-carburized

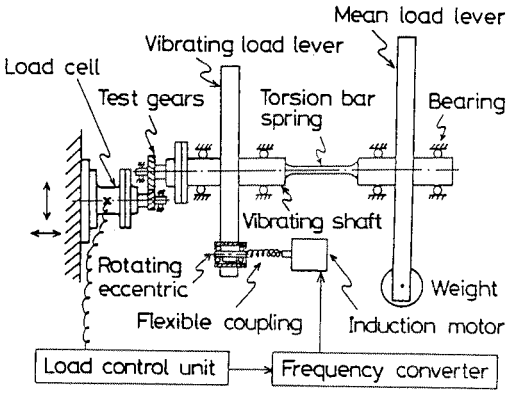

Fig. 2
Schematic of resonance type gear fatigue tester.

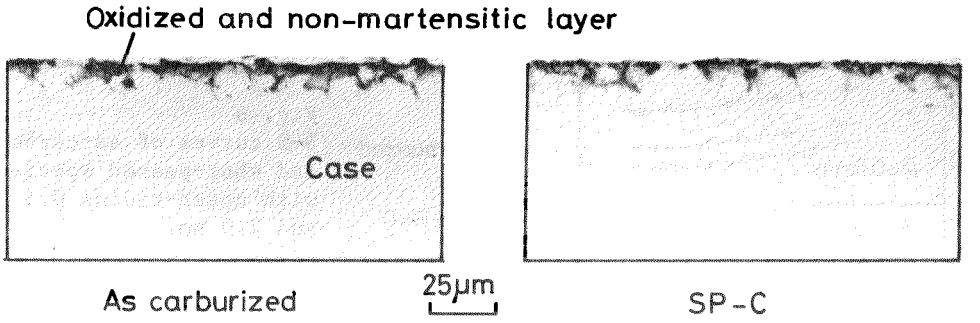

Fig. 3 Photomicrographs of surface layer of specimens, as-carburized and shot-peened under condition SP-C.

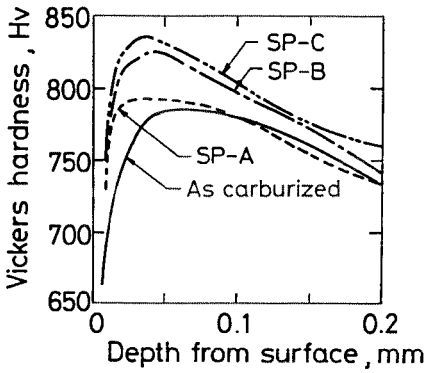

Fig. 4
Hardness distributions of as-carburized and shot-peened specimens with notch-radius 1.0 mm.

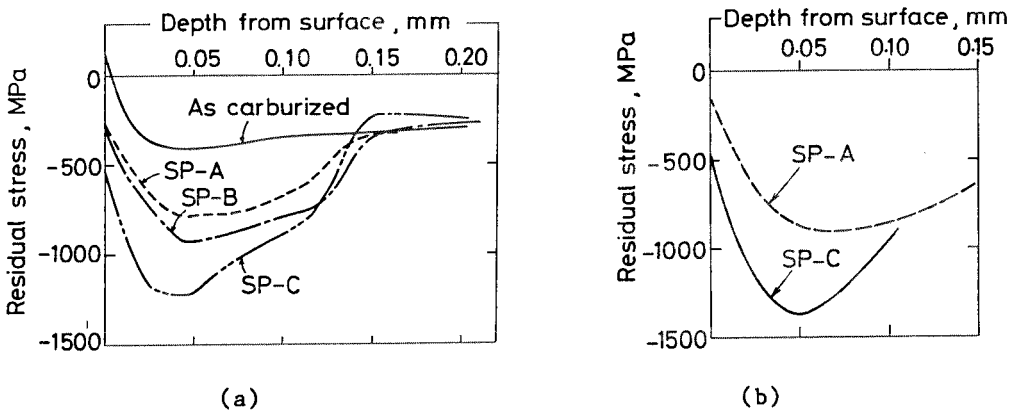

Fig. 5 Residual stress distributions of (a) as-carburized and shot-peened specimens with notch-radius 1.0 mm and (b) gears.

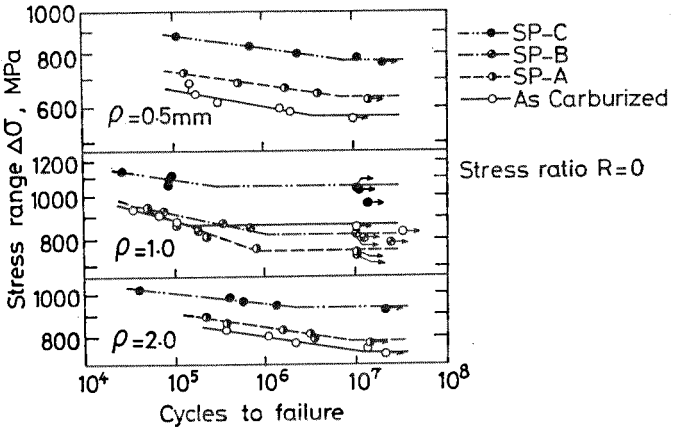

Fig. 6
S-N curves of as-carburized and shot-peened specimens with notch-radius 0.5, 1.0, and 2.0 mm.

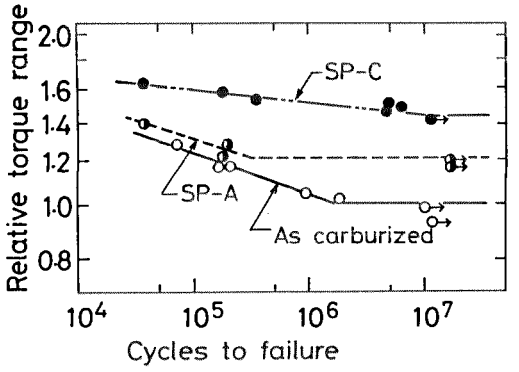

Fig. 7
S-N curves of as-carburized and shot-peened gears.

specimens do not correlate with the residual stress along the same regression line as those of the shot-peened specimens. The difference of regression line between the as-carburized and shot-peened specimens seems to be related to the difference in fracture mode: The former is a mixed mode of granular and transgranular fractures, whereas the latter has transgranular fractures, as shown in Fig. 9.
The fatigue limits of shot-peened specimens with different notch radiuses individually correlated to different regression lines. The fatigue limits of notched specimens are comprehensively explained hereafter, using a simple model based on the critical depth criterion[10]. The stress distribution in depth at the notch root with a stress concentration factor Kt, under a nominal bending stress σn, is illustrated in Fig. 10. The maximum stress σmax at the surface is

$$\sigma max = Kt \cdot \sigma n \tag{1}$$

and the stress gradient χ near the surface is

$$\chi = \frac{1}{\sigma max} \cdot \frac{d\sigma}{dx} = \frac{2}{\rho} + \frac{2}{d} \tag{2}$$

where ρ is the notch radius, and d is the specimen thickness.
According to the critical depth criterion, the effective stress σeff at the depth Δt from the surface correlated to the fatigue limits of the notched specimens, as can be expressed as follows:

$$\sigma eff = \sigma max \cdot (1 - \chi \cdot \Delta t) \tag{3}$$

It is generally recognized that particular Δt values exist according to the material states[10,11]. Therefore, the Δt value for the shot-peened notched specimens was estimated. The correlation coefficient between the σeff of fatigue limits and the residual stresses at the depth of Δt were calculated in the Δt range of 0.02 - 0.06 mm.
Figure 11 shows the result of this calculation. The correlation coefficient is at maximum when Δt = 0.05 mm. Fig. 12 shows the relation between the σeff at the fatigue limit and the residual stress when Δt = 0.05 mm. The experimental results of the shot-peened specimens and gears were within the ±5% scattering band of linear regression line. The gradient of the regression line is 0.63. The as-carburized specimens showed the behavior different from that of the shot-peened specimens shown in Fig. 8. Consequently, the fatigue limits of shot-peened gears and specimens with notches are strongly influenced by the residual stress distributions from the surface to the depth of 0.05 mm.
On the other hand, the critical depth of 0.05 mm corresponds with the sum of the maximum thickness of the oxidized and non-martensitic layer and a single grain size of prior austenite. The oxidized and non-martensitic layer has low hardness. Therefore, it is considered that this layer is damaged even by the cyclic stresses lower than the fatigue limit. The observation by the replication technique showed some micro-cracks on the surface near the notch root of the as-carburized and shot-peened specimens which endured 10^7 stress cycles below the fatigue limit. Fig. 13 shows an example of these micro cracks. The depths of the micro-cracks were 0.01 - 0.04 mm. The observation indicates that the fatigue limits of these specimens are determined by the retardation of micro-crack propagation, which is related to the correlation between the fatigue limits of shot-peeded specimens and the residual stress within 0.05 mm from the surface.

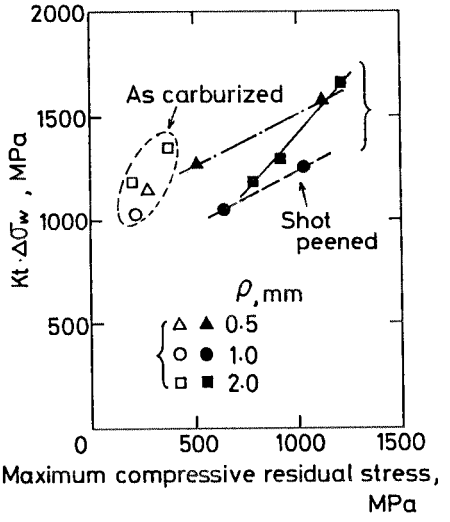

Fig. 8
Relation between Kt·Δσw and maximum compressive residual stress for as-carburized and shot-peened specimens with different notch-radiuses.

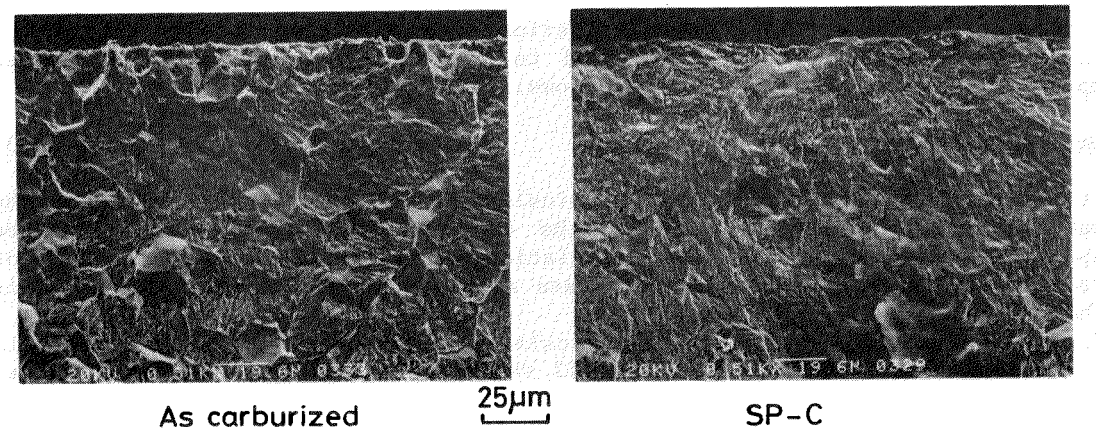

Fig. 9 SEM photographs of fracture surfaces around crack initiation point for specimens as-carburized and shot-peened under condition SP-C

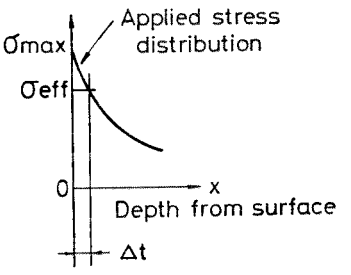

Fig. 10
Representation of applied stress distribution, critical depth Δt and effective stress σeff.

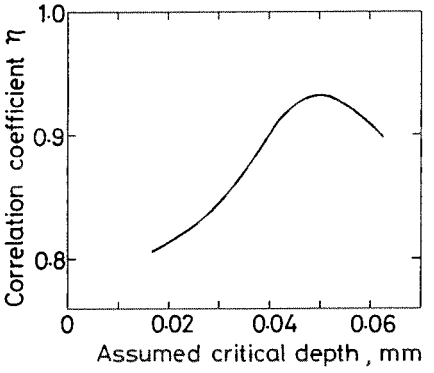

Fig. 11
Determination of critical depth Δt with correlation coefficient η between effective stress for fatigue limit and residual stress at assumed critical depth.

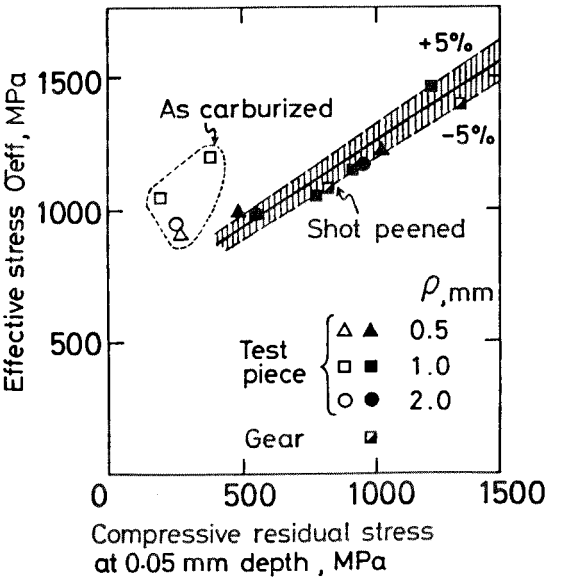

Fig. 12
Relation between effective stress for fatigue limit and residual stress at Δt of 0.05 mm.

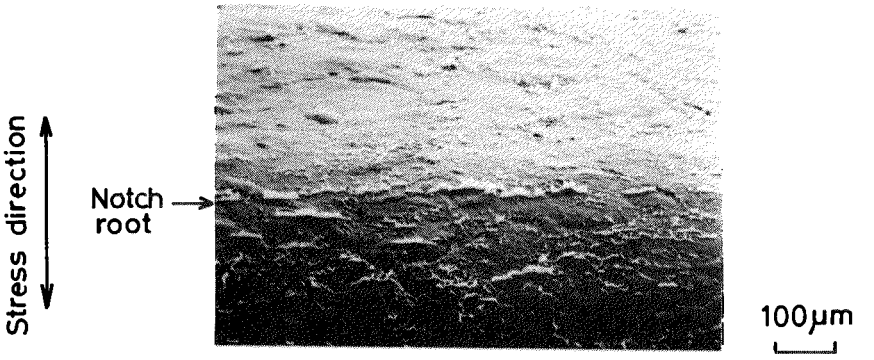

Fig. 13 SEM photograph of 1st stage replica of micro-cracks observed around the notch root of specimen endured 10^7 stress cycles.

CONCLUSIONS

1. The bending fatigue strengths of the gears and notched specimens which were shot-peened without machining after carburizing were strongly affected by the residual stress induced by shot peening.
2. The relation between the fatigue limits and the residual stresses of the shot-peened notched specimens was examined using a simple model based on the critical depth criterion. When the critical depth was assumed to be 0.05 mm, the fatigue limits of the specimens correlated well with the residual stresses.
3. The fatigue limits of the as-carburized specimens showed the behavior for the residual stress different from those of the shot-peened specimens.

REFERENCES

[1] McCormick, D. Design Engineering, Vol.52, No.7, pp.49-54 (July 1981)
[2] Hisamatu, S., et al. Isuzu Tech. Journal, No.63, pp.18-21 (1979)
[3] Burrell, N. K. SAE paper 850365 (1985)
[4] Miwa, Y., et al. SAE paper 880666 (1988)
[5] Schreiber, R., et al. Arch. Eisenhüttenwesen, Vol.49, No.5, pp.265-269 (1978)
[6] Hirsch, T. and Wohlfahrt, H. Antriebstechnik, Vol.25, No.9, pp.73-80 (1986)
[7] Komine, A., et al. Trans. of Jpn. Soc. of Mech. Eng., Vol.53, No.488, A, pp.702-708 (1987)
[8] Hoffman, J. E., et al. Proc. of Third Int. Conf. on Shot Peening, p.631 (1987)
[9] Ogawa, K., et al. Trans. of Jpn. Soc of Mech. Eng., Vol.53, No.485, C, pp.171-175 (1987)
[10] Ishibashi, T. Kinzoku no Hirou to Hakai no Boshi, Yokendo, Tokyo, 1967
[11] Flavenot, J. F. and Skalli, N. Life Assessment of Dynamically Loaded Materials and Structures, Vol.1, pp.335-344 (1984)